Supplemental data

$Na_V1.1$ inhibition can reduce visceral hypersensitivity

Juan Salvatierra, Joel Castro, Andelain Erickson, Qian Li, Joao Braz, John Gilchrist, Luke Grundy, Grigori Y. Rychkov, Annemie Deiteren, Rana Rais, Glenn F. King, Barbara S. Slusher, Allan Basbaum, Pankaj J Pasricha, Stuart M. Brierley, Frank Bosmans

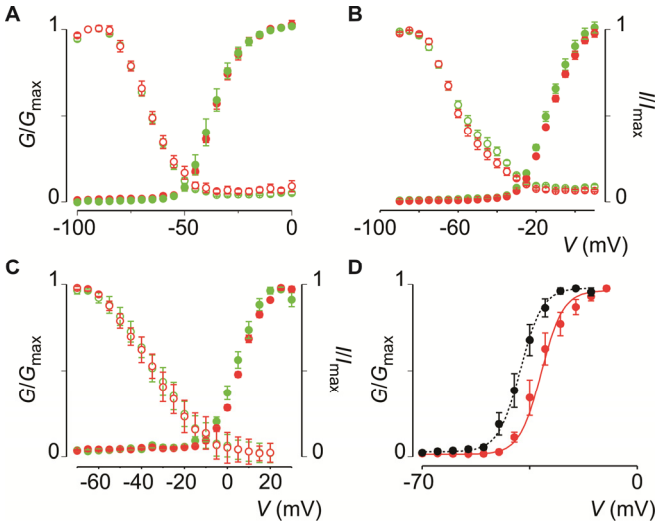

Supplementary Figure 1: Effect of 100µM Compound B on $Na_V1.5$, $Na_V1.7$, and $Na_V1.8$

A-C) Figure shows G/G_{max} (G: conductance) and I/I_{max} (I: current) relationships before (green, DMSO control) and after (red) addition of 100µM Compound B to $Na_V1.5$ (A), $Na_V1.7$ (B), and $Na_V1.8$ (C). n=5–8, and error bars represent SEM. No effects were observed. **D)** Effect of 1µM Compound B (red) on $Na_V1.1$ (black; control) activation voltage.

A

	Mouse	Mouse Microsomes		Human	Human Microsomes		Testo* (Mouse)	Testo* (Human)
Time	*Plasma*	*Phase I*	*Negative Control*	*Plasma*	*Phase I*	*Negative Control*	*Phase I*	*Phase I*
0	100%	100%	100%	100%	100%	100%	100%	100%
30	93%	97%	96%	103%	111%	107%	4%	21%
60	***93%***	***98%***	***96%***	***85%***	***110%***	***108%***	***0%***	***8%***

B

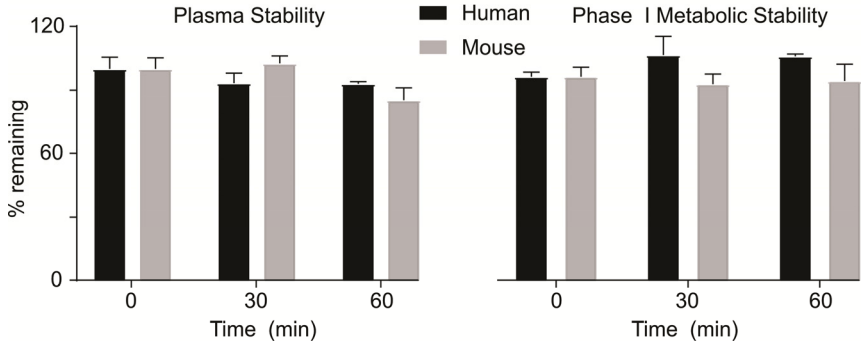

Supplementary Figure 2: Metabolic stability of Compound B in plasma and liver microsomes

Compound B was completely stable in both plasma as well as microsomes from mouse and human fortified with NADPH suggesting that the compound is not susceptible to hydrolysis or CYP-450 dependent metabolism. * Testosterone (Testo) was used as a positive control.

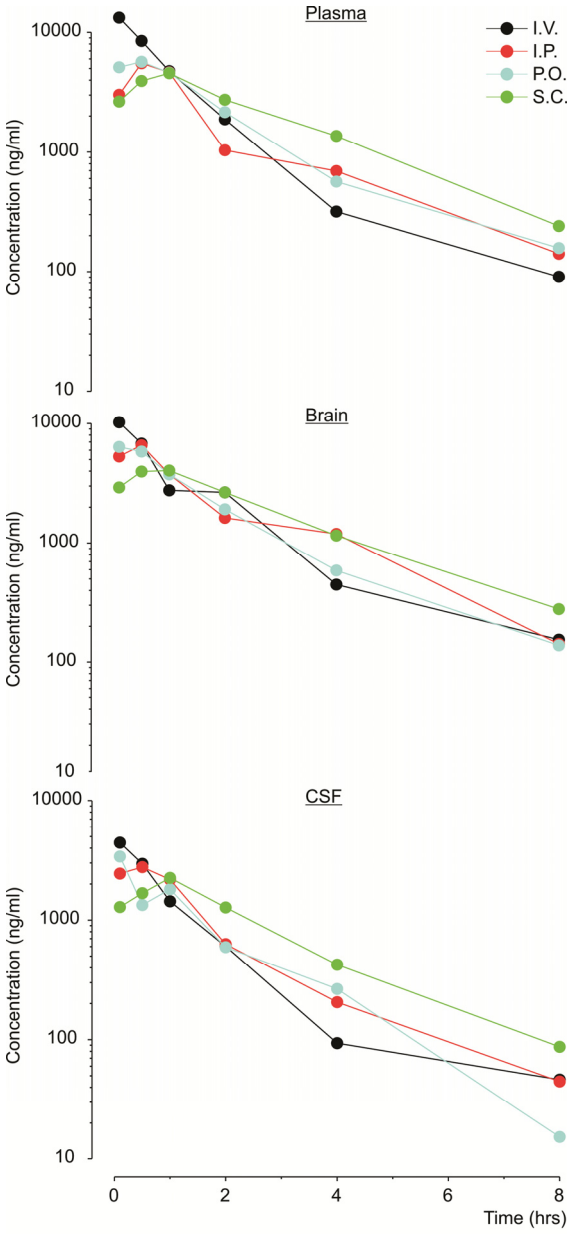

Supplementary Figure 3: Pharmacokinetic (PK) profile of Compound B

Figure shows mean concentration (ng/ml) – time (hrs) profiles of plasma, brain, and CSF (cerebrospinal fluid) pharmacokinetics of Compound B in male C57BL/6 mice following a single intravenous (I.V.), intraperitoneal (I.P.), subcutaneous (S.C.), and oral (P.O.) dose administration at 10mg/kg with 6 time points over 8hrs. Deduced values are shown in Supplementary Table 2.

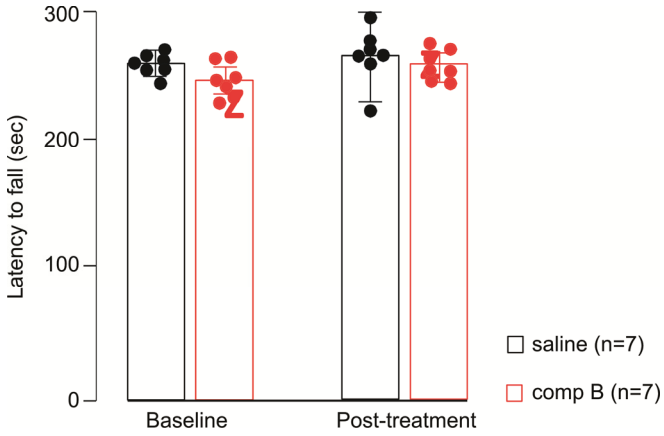

Supplementary Figure 4: Compound B assessment in the rotarod test

Systemic administration of Compound B (I.P., 60mg/kg) has no effect on motor performance on the rotarod test (baseline: 256sec ± 5 *vs* Compound B: 261sec ± 4, two-way ANOVA, p=0.990, n=7).

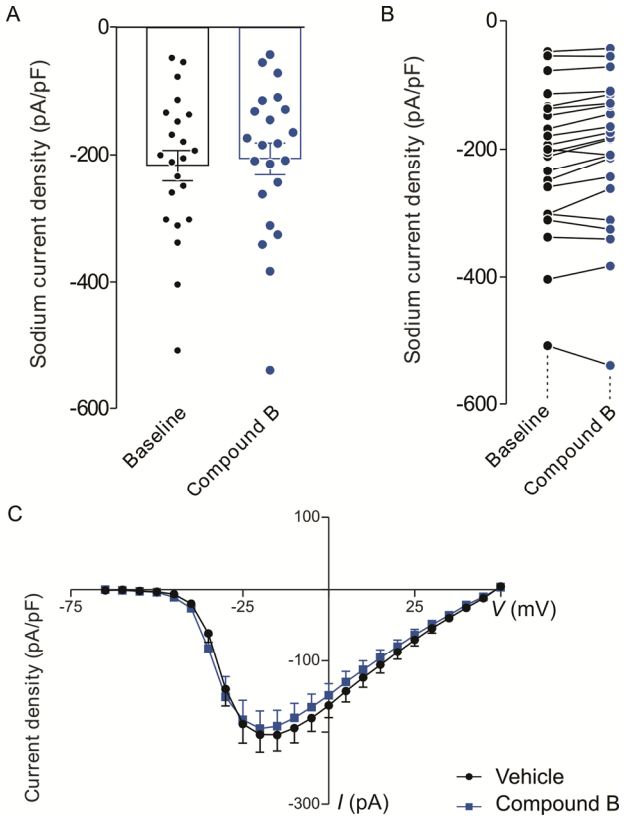

Supplementary Figure 5: Compound B does not affect sodium currents in a subpopulation of colon-innervating DRG neurons

A) Group data showing that sodium current density (pA/pF) in a population of colon innervating DRG neurons was not inhibited (defined as a ≥15% reduction from baseline responses) by Compound B ($p>0.05$, n=22 neurons, paired t-test). **B)** Individual data from the group data presented in A). **C)** *I-V* (current-voltage) plots of sodium current density before (vehicle; black) and after (blue) Compound B application (100µM) in uninhibited colon innervating DRG neurons.

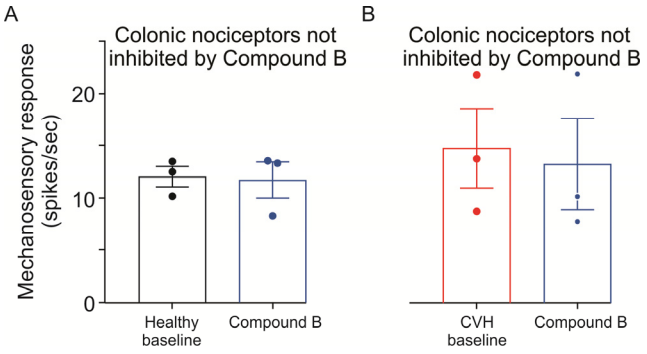

Supplementary Figure 6: Compound B does not affect a subpopulation of colonic nociceptive afferents from healthy control and CVH mice

A) Healthy control mice: application of Compound B (100µM) did not inhibit a population of nociceptors (n=3, p>0.05, paired t-test). **B)** TNBS colitis-induced CVH mouse model of IBS: application of Compound B (100µM) did not inhibit a population of CVH nociceptors (n=3, p>0.05, paired t-test).

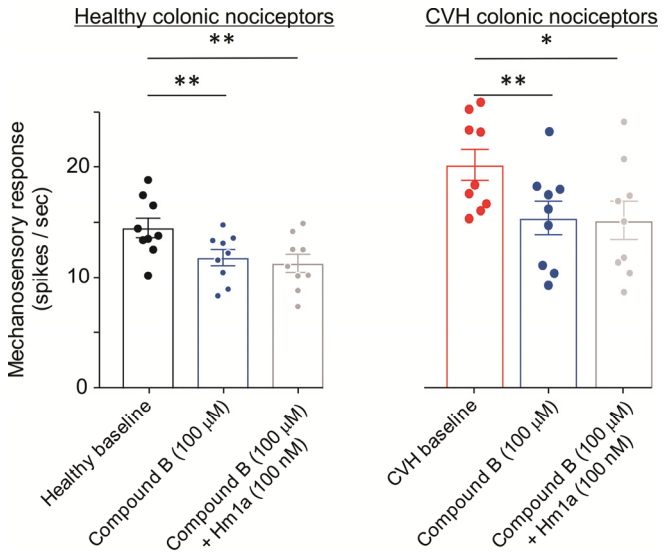

Supplementary Figure 7: Effect of Compound B and Hm1a on colonic nociceptive afferents

Left: Healthy control mice with application of 100µM Compound B inhibiting colonic nociceptors from control mice (n=9 afferents). Addition of 100nM Hm1a does not overcome Compound B inhibition. **Right:** In a TNBS colitis-induced CVH mouse model of IBS, application of Compound B inhibited colonic nociceptors from CVH mice (n=9 afferents). Co-application of 100nM Hm1a does not overcome Compound B inhibition. * $p<0.05$; ** $p<0.01$, repeated measures one-way ANOVA.

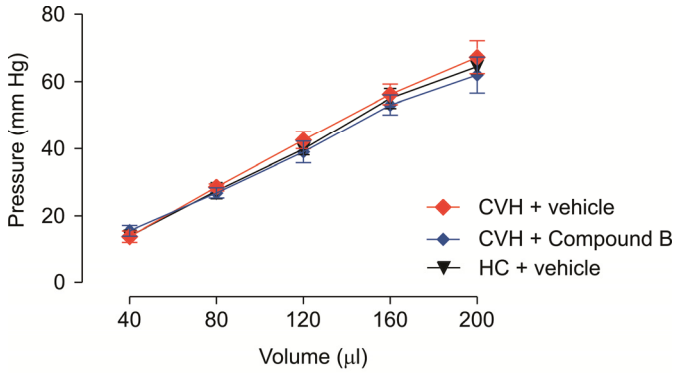

Supplementary Figure 8: Colonic compliance

Compared with healthy control mice, colonic compliance is unaltered in a TNBS colitis-induced CVH mouse model of IBS or IBS mice dosed with 100µM Compound B, suggesting that changes in the VMR to CRD are not due to changes in smooth muscle function. HC = Healthy Control.

Supplementary Table 1

Assay	Source	Ligand	Conc.	Kd	Non-specific	Incubation	Detection method	Result
Receptors								
A_{2A} (h) (agonist radioligand)	human recombinant (HEK-293)	[^{3}H]CGS 21680	6nM	27nM	NECA (10 µM)	120min RT	Scintillation counting	Negative
α1A (h) (antagonist radioligand)	human recombinant (CHO)	[^{3}H]prazosin	0.1nM	0.1nM	epinephrine (0.1mM)	60min RT	Scintillation counting	Negative
$α_{2A}$ (h) (antagonist radioligand)	human recombinant (CHO)	[^{3}H]RX 821002	1nM	0.8nM	epinephrine (100µM)	60min RT	Scintillation counting	Negative
$β_1$ (h) (agonist radioligand)	human recombinant (HEK-293)	[^{3}H](-)CGP 12177	0.3nM	0.39nM	alprenolol (50µM)	60min RT	Scintillation counting	Negative
$β_2$ (h) (antagonist radioligand)	human recombinant (CHO)	[^{3}H](-)CGP 12177	0.3nM	0.15nM	alprenolol (50µM)	120min RT	Scintillation counting	Negative
CB_1 (h) (agonist radioligand)	human recombinant (CHO)	[^{3}H]CP 55940	0.5nM	3.5nM	WIN 55212-2 (10µM)	120min 37°C	Scintillation counting	Negative
CB_2 (h) (agonist radioligand)	human recombinant (CHO)	[^{3}H]WIN 55212-2	0.8nM	1.5nM	WIN 55212-2 (5 µM)	120min 37°C	Scintillation counting	Negative
CCK_1 (CCK_A) (h) (agonist radioligand)	human recombinant (CHO)	[^{125}I]CCK-8s	0.08nM	0.24nM	CCK-8s (1µM)	60min RT	Scintillation counting	Negative
D_1 (h) (antagonist radioligand)	human recombinant (CHO)	[^{3}H]SCH 23390	0.3nM	0.2nM	SCH 23390 (1µM)	60min RT	Scintillation counting	Negative
D_{2S} (h) (agonist radioligand)	human recombinant (HEK-293)	[^{3}H]7-OH-DPAT	1nM	0.68nM	butaclamol (10µM)	60min RT	Scintillation counting	Negative
ET_A (h) (agonist radioligand)	human recombinant (CHO)	[^{125}I]endothelin-1	0.03nM	0.03nM	endothelin-1 (100nM)	120min 37°C	Scintillation counting	Negative
H_1 (h) (antagonist radioligand)	human recombinant (HEK-293)	[^{3}H]pyrilamine	1nM	1.7nM	pyrilamine (1µM)	60min RT	Scintillation counting	Negative
H_2 (h) (antagonist radioligand)	human recombinant (CHO)	[^{125}I]APT	0.075nM	2.9nM	tiotidine (100µM)	120min RT	Scintillation counting	Negative
M_1 (h) (antagonist radioligand)	human recombinant (CHO)	[^{3}H]pirenzepine	2nM	13nM	atropine (1µM)	60min RT	Scintillation counting	Negative
M_2 (h) (antagonist radioligand)	human recombinant (CHO)	[^{3}H]AF-DX 384	2nM	4.6nM	atropine (1µM)	60min RT	Scintillation counting	Negative
M_3 (h) (antagonist radioligand)	human recombinant (CHO)	[^{3}H]4-DAMP	0.2nM	0.5nM	atropine (1µM)	60min RT	Scintillation counting	Negative
N neuronal α4β2 (h) (agonist radioligand)	SH-SY5Y cells (human recombinant)	[^{3}H]cytisine	0.6nM	0.3nM	nicotine (10µM)	120min 4°C	Scintillation counting	Negative
δ (DOP) (h) (agonist radioligand)	human recombinant (CHO)	[^{3}H]DADLE	0.5nM	0.73nM	naltrexone (10µM)	120min RT	Scintillation counting	Negative
κ (KOP) (agonist radioligand)	rat recombinant (CHO)	[^{3}H]U 69593	1nM	2nM	naloxone (10µM)	60min RT	Scintillation counting	Negative
µ (MOP) (h) (agonist radioligand)	human recombinant (HEK-293 cells)	[^{3}H]DAMGO	0.5nM	0.35nM	naloxone (10µM)	120min RT	Scintillation counting	Negative
5-HT_{1A} (h) (agonist radioligand)	human recombinant (HEK-293)	[^{3}H]8-OH-DPAT	0.5nM	0.5nM	8-OH-DPAT (10µM)	60min RT	Scintillation counting	Negative
5-HT_{1B} (antagonist radioligand)	rat cerebral cortex	[^{125}I]CYP (+ 30µM isoproterenol)	0.1nM	0.16nM	serotonin (10µM)	120min 37°C	Scintillation counting	Negative
5-HT_{2A} (h)	human	[^{125}I](±)DOI	0.1nM	0.3nM	(±)DOI	60min RT	Scintillation	Negative

(agonist radioligand)	recombinant (HEK-293)				(1µM)		counting	
5-HT$_{2B}$ (h) (agonist radioligand)	human recombinant (CHO)	[^{125}I](±)DOI	0.2nM	0.2nM	(±)DOI (1µM)	60min RT	Scintillation counting	Negative
GR (h) (agonist radioligand)	IM-9 cells (cytosol)	[^{3}H]dexamethasone	1.5nM	1.5nM	Triamcinolone (10µM)	6hr 4°C	Scintillation counting	Negative
AR (h) (agonist radioligand)	LNCaP cells (cytosol)	[^{3}H]methyltrienolone	1nM	0.8nM	testosterone (1µM)	24hr 4°C	Scintillation counting	Negative
V$_{1a}$(h) (agonist radioligand)	human recombinant (CHO)	[^{3}H]AVP	0.3nM	0.5nM	AVP (1µM)	60min RT	Scintillation counting	Negative
Ion channels								
BZD (central) (agonist radioligand)	rat cerebral cortex	[^{3}H]flunitrazepam	0.4nM	2.1nM	diazepam (3µM)	60min 4°C	Scintillation counting	Negative
NMDA (antagonist radioligand)	rat cerebral cortex	[^{3}H]CGP 39653	5nM	23nM	L-glutamate (100µM)	60min 4°C	Scintillation counting	Negative
5-HT$_3$ (h) (antagonist radioligand)	human recombinant (CHO)	[^{3}H]BRL 43694	0.5nM	1.15nM	MDL 72222 (10µM)	120min RT	Scintillation counting	Negative
Ca^{2+} channel (L, dihydropyridine) (antagonist radioligand)	rat cerebral cortex	[^{3}H]nitrendipine	0.1nM	0.18nM	nitrendipine (1µM)	90min RT	Scintillation counting	Negative
Potassium channel hERG (human)-[^{3}H] Dofetilide	human recombinant (HEK-293)	[^{3}H] Dofetilide	3nM	6.6nM	Terfenadine (25µM)	60min RT	Scintillation counting	Negative
K$_V$ channel (antagonist radioligand)	rat cerebral cortex	[^{125}I]α-dendrotoxin	0.01nM	0.04nM	α-dendrotoxin (50nM)	60min RT	Scintillation counting	Negative
Transporters								
Norepinephrine transporter (h) (antagonist radioligand)	human recombinant (CHO)	[^{3}H]nisoxetine	1nM	2.9nM	desipramine (1µM)	120min 4°C	Scintillation counting	Negative
dopamine transporter (h) (antagonist radioligand)	human recombinant (CHO)	[^{3}H]BTCP	4nM	4.5nM	BTCP (10µM)	120min 4°C	Scintillation counting	Negative
5-HT transporter (h) (antagonist radioligand)	human recombinant (CHO)	[^{3}H]imipramine	2nM	1.7nM	imipramine (10µM)	60min RT	Scintillation counting	Negative
Enzymes								
MAO-A (antagonist radioligand)	rat cerebral cortex	[^{3}H]Ro 41-1049	10nM	14nM	clorgyline (1µM)	60 min 37°C	Scintillation counting	Negative
Kinases and other enzymes								
Assay	**Source**	**Substrate/stimulus/ tracer**			**Incubation**	**Measured component**	**Detection method**	**Result**
Lck kinase (h)	human recombinant (Sf9 cells)	ATP + Ulight-Poly GAT[EAY(1:1:1)]n (25nM)			10 min RT	phospho-Ulight-Poly GAT[EAY(1:1:1)]n	LANCE	Negative
COX1 (h)	human recombinant	Arachidonic acid (3µM) + ADHP (25µM)			3min RT	Resorufin (oxydized ADHP)	Fluorimetry	Negative
COX2 (h)	human recombinant (Sf9 cells)	Arachidonic acid (2µM) + ADHP (25µM)			5min RT	Resorufin (oxydized ADHP)	Fluorimetry	Negative
PDE3A (h)	human recombinant (Sf9 cells)	[^{3}H]cAMP + cAMP (0.5µM)			20min RT	[^{3}H]5'AMP	Scintillation counting	Negative
PDE4D2 (h)	human	[^{3}H]cAMP + cAMP (0.5µM)			20min RT	[^{3}H]5'AMP	Scintillation	Positive

	recombinant (Sf9 cells)				counting	
acetylcholin esterase (h)	human recombinant (HEK-293)	Acetylthiocholine (400µM)	30min RT	5 thio 2 nitrobenzoic acid	Photometry	Negative

Supplementary Table 2

Route	Matrix	T_{max} (hrs)	C_0/C_{max} (ng/ml)	AUC_{last} (ng*hr/ml)	AUC_{inf} (ng*hr/ml)	$T_{1/2}$ (hrs)	CL (ml/min/kg)	Vss (l/kg)	% F[a]
I.V.	Plasma	-	14442	15319	15479	1.4	10.8	0.8	-
	Brain[b]	-	11116	13861	14151	1.6	11.8	1.1	-
	CSF	-	4795	5016	5111	1.8	32.1	2.5	-
I.P.	Plasma	0.5	5523	10694	11134	-	-	-	-
	Brain[b]	0.5	6579	13505	13878	-	-	-	-
	CSF	0.5	2776	5179	5277	-	-	-	-
P.O.	Plasma	0.5	5681	12097	12437	-	-	-	79
	Brain[b]	0.25	6371	11525	11828	-	-	-	-
	CSF	0.25	3397	4426	4453	-	-	-	-
S.C.	Plasma	1.00	4570	14237	14839	-	-	-	-
	Brain[b]	1.00	4041	14010	14010	-	-	-	-
	CSF	1.00	2248	6190	6190	-	-	-	-

PK data (see Supplementary Fig. 3):
[a] AUC_{last} was used for bioavailability calculation.
[b] Brain concentration and exposure expressed as ng/g and ng/g*hr, density of brain tissue was considered to be 1 which is equivalent to plasma density.